Emergence of ferromagnetism and Jahn-Teller distortion in LaMn1–xCrxO3 (x

Aline Y. Ramos, Hélio Tolentino, Marcio Soares, Stéphane Grenier, Oana Bunau, Yves Joly, Francois Baudelet, Fabrice Wilhelm, Andrei Rogalev, Narcizo M. Souza-Neto, et al.

PHYSICAL REVIEW B **87**, 220404(R) (2013)

Emergence of ferromagnetism and Jahn-Teller distortion in $LaMn_{1-x}Cr_xO_3$ ($x < 0.15$)

Aline Y. Ramos,[1,*] Hélio C. N. Tolentino,[1] Márcio M. Soares,[1] Stéphane Grenier,[1] Oana Bunău,[1] Yves Joly,[1] François Baudelet,[2] Fabrice Wilhelm,[3] Andrei Rogalev,[3] Raquel A. Souza,[4] Narcizo M. Souza-Neto,[4] Olivier Proux,[5] Denis Testemale,[1] and Alberto Caneiro[6]

[1]*Institut Néel, CNRS and UJF, Boîte Postale 166, F-38042 Grenoble Cedex 9, France*
[2]*Synchrotron SOLEIL, L'Orme des Merisiers, Saint-Aubin, Boîte Postale 48, 91192 Gif-sur-Yvette Cedex, France*
[3]*European Synchrotron Radiation Facility–ESRF, F-38043 Grenoble, France*
[4]*Laboratório Nacional de Luz Síncrotron, P.O. Box 6192, 13084-971 Campinas, São Paulo, Brazil*
[5]*Observatoire des Sciences de l'Univers–OSUG–Grenoble, F-38051 Grenoble, France*
[6]*Centro Atómico Bariloche, CNEA and Universidad Nacional de Cuyo, 8400 S.C. de Bariloche, Argentina*

(Received 1 February 2013; revised manuscript received 23 May 2013; published 10 June 2013)

The emergence of a ferromagnetic component in $LaMnO_3$ with low Cr-for-Mn substitution has been studied by x-ray absorption spectroscopy and x-ray magnetic circular dichroism at the Mn and Cr K edges. The local magnetic moment strengths for Mn and Cr are proportional to each other and follow the macroscopic magnetization. The net ferromagnetic components of Cr^{3+} and Mn^{3+} are found antiferromagnetically coupled. Unlike hole doping by La site substitution, the inclusion of Cr^{3+} ions up to $x = 0.15$ does not decrease the Jahn-Teller (JT) distortion and consequently does not significantly affect the orbital ordering. This demonstrates that the emergence of the ferromagnetism is not related to JT weakening and likely arises from a complex orbital mixing.

DOI: 10.1103/PhysRevB.87.220404 PACS number(s): 75.25.−j, 71.70.Ej, 75.30.Et, 78.70.Dm

Doped manganites have been extensively studied owing to their colossal magnetoresistance property and its potential applications to magnetic devices. The substitution at the Mn site (B site in the ABO_3 perovskite formula) of various transition-metal elements dramatically modifies the magnetic and electronic properties. The variations of the magnetic and electronic behaviors are associated with the dissimilar $3d$ electron configuration of the substitutions. Cr doping at the Mn sites has attracted special attention because Cr^{3+} ions have the same electronic configuration $t_{2g}^3 e_g^0$ as Mn^{4+}. As the Cr^{3+} ionic radius (0.615 Å) is much closer to that of Mn^{3+} high spin (0.645 Å) than Mn^{4+} radius (0.530 Å), low substitutions of Cr^{3+} result in changing the Mn^{3+} density without large distortion of the crystal cell.[1] These features make the partial substitution of Mn by Cr in $LaMnO_{3.00+\delta}$ an interesting system for studying the close relationship between Jahn Teller (JT) distortion, double exchange (DE), and superexchange (SE) interactions and orbital degeneracy. Since the first studies of the series $LaMn_{1-x}Cr_xO_3$ in the 1950s,[2,3] it is known that upon Cr doping the antiferromagnetic (AFM) Mott insulator $LaMnO_3$ develops a ferromagnetic (FM) component, but the character of the Mn^{3+}-Cr^{3+} interaction has been under debate for a long time.[1,2,4–16] A Mn^{3+}-Cr^{3+} SE FM coupling may account for the increasing Curie temperature and spontaneous magnetization with increasing Cr doping.[4–7] On the other hand, several groups proposed DE interaction between Mn^{3+} and Cr^{3+}.[1,7] Cr dopants can also be viewed as a quenched random field.[8,9] However, direct x-ray magnetic circular dichroism experiments suggest that the exchange interaction between Mn^{3+} and Cr^{3+} leads to a net local antiparallel coupling,[12–15] regardless of the magnetic state nature of the manganite compound. This scenario is supported by spin resonance investigations.[16]

The local distortion in Cr-substituted systems has not yet been the object of a specific study. The usual view is that, in a similar way as the formal introduction of Mn^{4+} by A-site doping and/or oxygen overstoichiometry, B-site Cr^{3+} substitution weakens the cooperative JT distortion, and consequently affects the orbital order and favors the onset of FM ordering. In contrast to this scenario where local site symmetrization drives the magnetic behavior, Zhou *et al.*[17] recently proposed that, for Ga-substituted doped manganites, local site distortions could bias the orbital ordering so as to make orbital mixing responsible for the three-dimensional (3D) ferromagnetism. In order to clarify the spin-spin interactions and ascertain the relative importance of removing a JT ion and of hole doping, we performed coupled magnetic and local structural studies by x-ray absorption near-edge spectroscopy (XANES) and x-ray magnetic circular dichroism (XMCD) at the transition metals K edge, in $LaMn_{1-x}Cr_xO_{3.00}$ with low substitution of Mn^{3+} by Cr^{3+}. We chose to study specifically the emergence of the FM component in Mn^{4+}-free compounds, with limited crystallographic distortions with respect to $LaMnO_3$. This series of compounds presents the double advantage of avoiding additional complexity due to Mn^{3+}-Mn^{4+} and Mn^{4+}-Cr^{3+} magnetic interactions, and the mixture of Mn^{3+} and Mn^{4+} local sites in mixed-valence compounds, and of starting from the parent compound $LaMnO_{3.00}$ where the local structure is well characterized.[18–21] The physics studied in our paper concerns then the first steps in the substitution of Mn atoms by Cr and is relatively simple because there are no Mn^{4+} ions and Cr^{3+}-Cr^{3+} interactions may be considered negligible.

In this Rapid Communication we show that the local magnetic moments at the Mn and Cr atoms are proportional to the ferromagnetic component in the macroscopic magnetization, and that their alignment is always antiparallel. We found that Cr is assimilated in the Mn network and that the Cr environment is essentially kept similar to that of Mn atoms, with no significant reduction in the distortion, even if Cr^{3+} is not a Jahn-Teller ion. This contradicts the usual guess[1,9,14]

and indicates that JT weakening is not responsible for the emergence of ferromagnetism, which should otherwise arise from orbital mixing.

Polycrystalline powdered $LaMn_{1-x}Cr_xO_3$ with $x = 0.05$, 0.1, and 0.15 (corresponding to 5%, 10%, and 15% of additional e_g holes)[22,23] and $LaMn_{0.90}Cr_{0.10}O_{3.04}$ (18% e_g holes, 8% being provided by oxygen overstoichiometry-Mn^{4+} ions)[24] were prepared by the liquid-mix method, using an experimental procedure elaborated to enable accurate control of the sample stoichiometry.[25] These compounds crystallize in the orthorhombic structure (*Pnma*). They keep the $LaMnO_3$ A-AFM spin structure, i.e., FM ordering in the *ab* planes and AFM between adjacent planes, but exhibit a significant ferromagnetic component along the *c* axis.[22,23] Room temperature (RT) XANES spectra at the Mn *K* edge (6539 eV) were collected in the transmission mode at the Brazilian Synchrotron Light Laboratory (LNLS) XAS1 beamline.[26] To check the strict stoichiometry of our samples, a XANES reference of metal foil was collected simultaneously. No edge shift is observed between the Mn^{4+}-free samples and the $LaMnO_3$ standard, within the precision of the experiments (0.1 eV). On the contrary, for the nonstoichiometric $LaMn_{0.90}Cr_{0.10}O_{3.04}$ sample, we observe an edge shift of ∼0.6 eV with respect to XANES of $LaMnO_3$, in agreement with the increase in the formal valence. RT XANES spectra at the Cr *K* edge (5989 eV) were collected at the French CRG–BM30B beamline at the European Synchrotron Radiation Facility (ESRF) using the fluorescence mode with a 30-element Ge solid state detector.[27] The energy resolution, including experimental resolution and core hole width, was about 1.5 eV at the Cr *K* edge and 2 eV at the Mn *K* edge. The XANES spectra were normalized, after background subtraction, at ∼200 eV above the edge for the Mn edge and 50 eV for the Cr edge. Coupled Mn and Cr *K*-edge XMCD measurements were performed at the ID12 beamline at the ESRF, using the total fluorescence yield mode with a Si photodiode detector and degree of circular polarization of the monochromatic beam of 88%. The samples were kept at 10 K and magnetized by applying a 3 T magnetic field. The temperature dependence of the Mn XMCD was studied at the ODE dispersive beamline at the synchrotron SOLEIL, using the transmission mode and a CCD detector.[28] The sample temperature was varied from 30 K to room temperature. XMCD spectra were recorded by reversing a permanent magnet of 1.1 T magnetic field and maintaining the polarization of the light, with a degree of circular polarization of ∼80%. The XMCD signals resulting from several scans were added and normalized to the absorption jump. Slight differences between the signals collected in the transmission (temperature dependent Mn *K* XMCD) and the fluorescence modes (coupled 10 *K* XMCD at Mn and Cr *K* edges) arise from differences in the amplitude of the contribution of La edge.[15] After subtraction of this contribution the spectral shape is the same in both cases and the XMCD amplitude is identical for a sample measured in the same conditions in the fluorescence and in the transmission mode.

Due to the selection rules in x-ray absorption spectroscopy, the *K*-edge transition originates from the core 1*s* state to the projected *np* (mainly 4*p*) unoccupied density of states (DOS). X-ray absorption probes the partial DOS modified

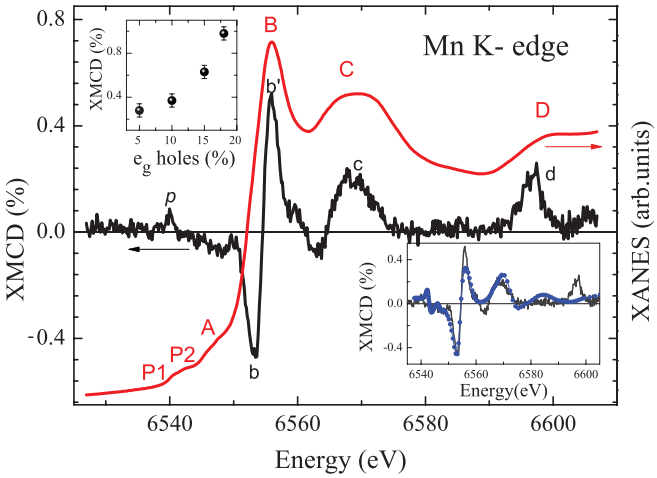

FIG. 1. (Color online) XANES and XMCD (10 K, 3 T) at the Mn *K* edge for $LaMn_{0.9}Cr_{0.1}O_{3.04}$. The value peak *b* to peak *b*′ is taken as a measure of the XMCD signal intensity. Top inset: XMCD signal as a function of the number of e_g holes. Lower inset: *ab initio* calculation of the XMCD signal (dots) compared to experimental (line).

by the presence of the 1*s* core hole that sorts out the 4*p* states around the Mn site from the ground state band structure. The XANES signal at the Mn *K* edge (Fig. 1) is dominated by a main line B, essentially related to the first coordination shell, followed by structures (C and D) arising from multiple scattering events. The pre-edge feature is formed by two peaks (P1, P2) and a shoulder (A) associated with transition from Mn 1*s* levels to 4*p* empty levels.[19,21,29] XMCD at the *K* edge of the transition metals probes the orbital polarization of the conduction *p* states, related to the spin polarization through the spin-orbit interaction.[30] Consequently, the XMCD at the *K* edge is, in its integral form, a measure of the orbital magnetism of the 4*p* shell of the transition metal probed by the x rays. The delocalized 4*p* states are coupled by exchange interaction with the spin-polarized 3*d* band, which dominates the magnetic properties of the system. Therefore the *K*-edge XMCD intensity is proportional to the orbital magnetic moment of the 3*d* bands.[31]

Ab initio calculations of the XANES and XMCD features were performed using the FDMNES code.[32] The electronic structure around the absorbing atoms is calculated using the multiple scattering theory within the muffin-tin approximation, based on a monoelectronic approach. The absorption is convoluted to a Lorentzian with an energy dependent width, to take into account the core and final state lifetimes and with a Gaussian to mimic the experimental energy resolution. Calculations are performed for clusters built from crystallographic data. In the Mn edge calculations we do not include Cr atoms in the cluster. The Cr edge XANES are calculated considering the only substitution of the Cr as the central atom of the cluster. Clusters of 33 atoms (radius 4.5 Å) are large enough to reproduce the XMCD features, while clusters up to 81 atoms (radius 6.5 Å) were required to reproduce all XANES and pre-edge features.[21] The spectral shape of the XMCD signal at the Mn *K* edge in our samples (Fig. 1) changes from negative to positive at the edge (*b, b*′); it shows a resonance (*c*) stemming from multiple scattering of magnetic

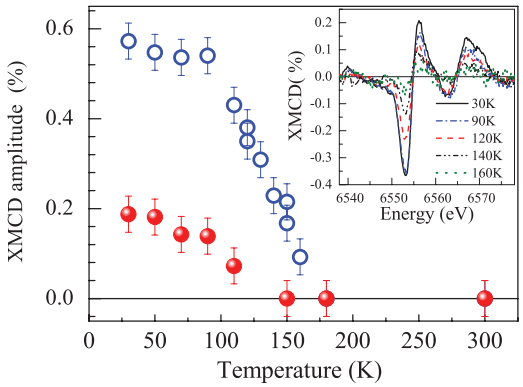

FIG. 2. (Color online) Temperature dependence (1.1 T) of the Mn K-edge XMCD amplitude (see text) for $LaMn_{0.9}Cr_{0.1}O_{3.04}$ (open circles) and $LaMn_{0.85}Cr_{0.15}O_{3.00}$ (full circles). Inset: XMCD signal of $LaMn_{0.9}Cr_{0.1}O_{3.04}$ at selected temperatures.

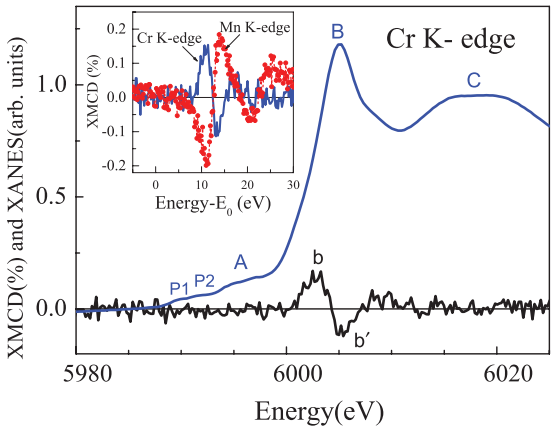

FIG. 3. (Color online) XANES and XMCD (30 K, 3 T) at the Cr K edge for $LaMn_{0.9}Cr_{0.1}O_{3.00}$. Inset: XMCD signals for $LaMn_{0.9}Cr_{0.1}O_{3.00}$ at the Cr K edge and Mn K edge. The two energy scales have been shifted to coincide at the main inflection point.

nearest neighbors, and finally a further peak (d) is observed, associated with simultaneous excitation of $3p$ electrons.[33] In the sample with the largest XMCD signal we also identify a resonance (p) in the pre-edge range. These spectral features are retained for all samples with only changes in the amplitudes. The XMCD amplitude is defined here by the peak to peak value (b, b'), relative to the edge jump. This amplitude increases as a function of the number of holes (Fig. 1, upper inset). All features are well reproduced by calculations (Fig. 1, lower inset), except for the peak d, confirming the multielectronic character of this structure.

As a first step, to relate the XMCD signal to the macroscopic magnetic properties,[22,23] we studied the temperature dependence of the Mn K edge XMCD for two samples $LaMn_{0.9}Cr_{0.10}O_{3.04}$ and $LaMn_{0.95}Cr_{0.15}O_{3.00}$. This dependence (Fig. 2) agrees with the ferromagnetic thermal evolution reported in these samples.[22,23] We observe, as in macroscopic measurements, a small reduction in the critical temperature in $LaMn_{0.95}Cr_{0.15}O_{3.00}$ with respect to $LaMn_{0.9}Cr_{0.10}O_{3.04}$. At 30 K and 1.1 T, the XMCD amplitude ratio between the two samples, i.e., the ratio between magnetic moment strengths at the Mn site, is about the ratio of the ferromagnetic component of the magnetic moment found by neutron scattering.

As concerns the Cr K edge (see Fig. 3 for the sample $LaMn_{0.9}Cr_{0.1}O_{3.00}$), the XMCD signal is opposite to that found at the Mn K edge (Fig. 3, inset), suggesting an antiferromagnetic Cr-Mn coupling. However, as the K-edge XMCD measures only the orbital part of the magnetic moment, conclusions about the direction of the net moment should be supported by calculations. The calculation at the Mn edge is made with a net positive magnetic moment (number of spins up $>$ number of spins down). This gives the correct shape and sign of the XMCD signal (Fig. 1, lower inset). At the Cr K edge, the calculations have been performed both for a net positive (number of spins up $>$ number of spins down) and a net negative magnetic moment (number of spins down $>$ number of spins up). The two calculations give the same shape but opposite signals. The Cr-XMCD signal that matches the experimental result is the one with a net negative magnetic moment. So, we can conclude that the net magnetic moments of Mn and Cr are opposite. The XMCD spectral shape and sign are retained for all samples with only changes in the amplitude. The coupling has the same antiferromagnetic character regardless if Mn^{4+} ions are present in the samples. This demonstrates that this coupling is essentially determined by Mn^{3+}-Cr^{3+} interactions.

We turn now to the characterization of the Cr^{3+} local environment. The EXAFS analysis of the Mn coordination shell gives the same parameters for $LaMnO_3$ and for all Mn^{4+}-free ($x = 0.05$, 0.10, and 0.15) samples. Similar results have been reported in Ga-substituted samples,[34] where a decrease of the JT distortion at the Mn sites is only observed by EXAFS analysis for $x \geqslant 0.2$. However, due to the high initial distortion of the Mn^{3+} sites in $LaMnO_3$, the EXAFS analysis has a limited sensitivity to small relaxations of the local distortion and this result is not conclusive. More convincing is the striking similarity between the XANES collected for the same sample at the Cr and Mn K edges [Fig. 4(a)], especially in pre-edge range [Fig. 4(a), inset]. This indicates that the Cr^{3+} ions in substitution in the $LaMnO_3$

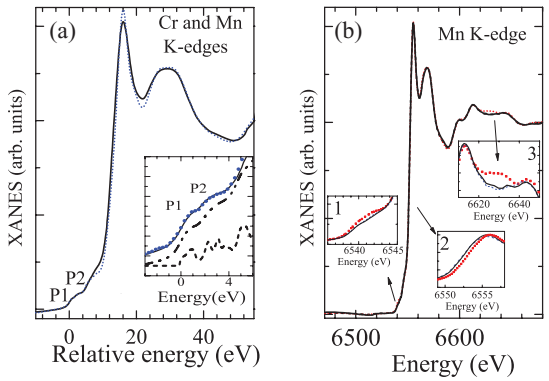

FIG. 4. (Color online) (a) XANES spectra at the Cr (dots) and Mn (plain line) K edges for the sample $LaCr_{0.1}Mn_{0.9}O_{3.0}$. The energy scales have been shifted to coincide at the first inflexion point. Inset: zoom in of the pre-edge range: the dashed lines correspond to *ab initio* calculations before and after convolution. (b) XANES spectra at the Mn K edge in $LaMnO_3$ (black plain line), $LaCr_{0.1}Mn_{0.9}O_{3.0}$(blue-dashed line), and $LaMnO_{3.05}$(red dots). The insets highlight the domains with spectral differences.

structure, adopt the same distorted local environment as the Mn^{3+} ions with negligible relaxation of the oxygen positions around them. This outcome is corroborated by a comparison [Fig. 4(b)] of the Mn K-edge XANES in $LaMnO_3$ to the XANES for two samples where 10% of e_g holes are introduced either by Cr^{3+} substitution ($LaCr_{0.1}Mn_{0.9}O_{3.0}$) or by oxygen overstoichiometry ($LaMnO_{3.05}$). In $LaMnO_{3.05}$ the pre-edge structure intensity is enhanced [Fig. 4(b), inset 1] and the edge jump is shifted towards higher energy due to the presence of Mn^{4+} ions [Fig. 4(b), inset 2]. An additional structure also emerges around 90 eV above the edge [Fig. 4(b), inset 3]. Such structure is due to multiple scattering and corresponds to an increase of the Mn-O-Mn angle, associated with the rupture of the orbital order.[19,21] These changes are the result of the symmetrization of the Mn environment when doping with the introduction of 10% of e_g holes (Mn^{4+}) by oxygen overstoichiometry. On the contrary, the introduction of 10% of e_g holes by Cr^{3+} substitution does not change the XANES spectrum, in either the pre-edge and edge-jump ranges, or around 90 eV above the edge [Fig. 4(b)], demonstrating that the Mn environment remains unchanged by Cr substitution. Unlike Mn^{4+}, Cr^{3+} substitution does not significantly alter the local site symmetry or the Mn-O-Mn superexchange angle. We conclude that the JT is not significantly weakened by substitution of Mn^{3+} by Cr^{3+} up to 15%. This agrees with the results obtained in Ga-substituted manganites for $x = 0.1$.[34] Nevertheless, while the nonmagnetic Ga^{3+} ion takes no part in the magnetic interactions, this is not the case for the magnetically active Cr^{3+} ion. It is worth emphasizing that Cr^{3+} substitutes Mn^{3+}, within the same local distorted environment, even though it has an important role in the magnetic interactions.

In low x $LaMn_{1-x}Cr_xO_3$ compounds the Cr^{3+}-Cr^{3+} interactions can be neglected in a first approximation. In these Mn^{4+}-free samples the spin configuration stems only from the competition of Mn^{3+}-Cr^{3+} and Mn^{3+}-Mn^{3+} interactions. We should remind one that in the parent compound A-AFM $LaMnO_3$, Mn^{3+}-Mn^{3+} interactions are of two different natures. The Mn^{3+} spins are coupled ferromagnetically within ab planes and and these planes are coupled antiferromagnetically along the c axis. Our experimental results can be understood within the scenario where the A-AFM order of $LaMnO_3$ is maintained, but with a small FM component along the c axis. When Cr^{3+}replaces one Mn^{3+} in the network it will also experience both types of interactions. Experimentally, we have shown that the signs of net magnetic moment of Mn^{3+} and Cr^{3+} ions are opposite. Moreover, the Cr^{3+} ions are substituted with Mn^{3+} ions at exactly the same sites, with no shift of oxygen towards Cr^{3+}. The Mn site distortion, e_g orbital occupancy, and spin order remain essentially unmodified, with an increase of the FM component along the c axis. As the Cr^{3+} ion has no e_g electron, hopping from the neighboring ions—and DE mechanism—becomes possible. Within the robust A-AFM scenario, this results in a largely frustrated spin configuration. In a possible configuration ferromagnetic DE between Cr and Mn magnetic moments is effective within the ab plane, but with an antiparallel alignment of the magnetic component along the c axis. Electron hopping along the c axis would be in this way less effective due to this antiparallel alignment and electrical conductivity would be highly anisotropic.

With a Cr magnetic moment aligned antiparallel to the Mn spins along the c axis, and parallel to the Mn spins in ab planes, the net FM moments of Cr and Mn are then proportional and opposite along the c axis. The highly frustrated magnetic arrangement is in agreement with the observation of Morales and co-workers[22] who found, for a same hole number, more magnetic frustration in $LaMn_{0.9}Cr_{0.1}O_3$ than in $LaMnO_{3.05}$. We should emphasize that the emergence of a FM component does not involve the same mechanism as A-site substitution, where the presence of Mn^{4+} decreases the cooperative JT distortion, thereby partially restoring the degenerescence of the e_g orbital and consequently weakening the orbital ordering. Our results rule out the decrease of the JT distortion as the factor weakening the antiferromagnetic Mn^{3+}-Mn^{3+} superexchange. Orbital mixing due to structural bias may likely play an important role.

In conclusion, we studied the emergence of the FM component with the inclusion of Cr^{3+} ions in $LaMnO_3$. The net magnetic moment of Cr^{3+} ions is antiparallel to the moments of the Mn^{3+} neighbors. Up to ∼15%, Cr to Mn substitution takes place without rupture of the orbital ordering, the Cr^{3+} ions occupying the Mn^{3+} sites without reduction of the local distortion. We ascertain that the mechanism of emergence of 3D FM is different from the usual A-site doping, when Mn^{4+} is formally introduced. Furthermore, our results emphasize the importance of local scale studies to safely characterize the spin-spin interactions in strongly correlated systems.

LNLS, SOLEIL, and ESRF synchrotrons are acknowledged for beam time.

*aline.ramos@grenoble.cnrs.fr

[1] L. Morales, R. Allub, B. Alascio, A. Butera, and A. Caneiro, Phys. Rev. B **72**, 132413 (2005).

[2] U. Bents, Phys. Rev. **106**, 225 (1957).

[3] G. Jonker, Physica **22**, 707 (1956).

[4] R. Ganguly, I. Gopalakrishnan, and J. Yakhmi, Physica B: Condensed Matter **275**, 308 (2000).

[5] R. Gundakaram, A. Arulraj, P. Vanitha, C. N. R. Rao, N. Gayathri, A. Raychaudhuri, and A. K. Cheetham, J. Solid State Chem. **127**, 354 (1996).

[6] Z. Qu, L. Pi, S. Tan, S. Chen, Z. Deng, and Y. Zhang, Phys. Rev. B **73**, 184407 (2006).

[7] Y. Sun, W. Tong, X. Xu, and Y. Zhang, Phys. Rev. B **63**, 174438 (2001).

[8] J. Farrell and G. A. Gehring, New J. Phys. **6**, 168 (2004).

[9] O. Cabeza, M. Long, C. Severac, M. A. Bari, C. M. Muirhead, M. G. Francesconi, and C. Greaves, J. Phys.: Condens. Matter **11**, 2569 (1999).

[10] A. Barnabe, A. Maignan, M. Hervieu, F. Damay, C. Martin, and B. Raveau, Appl. Phys. Lett. **71**, 3907 (1997).

[11]L. Capogna, A. Martinelli, M. G. Francesconi, P. G. Radaelli, J. Rodriguez Carvajal, O. Cabeza, M. Ferretti, C. Castellano, T. Corridoni, and N. Pompeo, Phys. Rev. B **77**, 104438 (2008).

[12]K. Ono, S. Nakazono, and M. Oshima, J. Magn. Magn. Mater. **226-230**, 869 (2001).

[13]O. Toulemonde, F. Studer, A. Barnabe, A. Maignan, C. Martin, and B. Raveau, Eur. Phys. J. B **4**, 159 (1998).

[14]H. Terashita, J. C. Cezar, F. M. Ardito, L. F. Bufaical, and E. Granado, Phys. Rev. B **85**, 104401 (2012).

[15]J. C. Cezar, N. M. Souza-Neto, C. Piamonteze, E. Tamura, F. Garcia, E. J. Carvalho, R. T. Neueschwander, A. Y. Ramos, H. C. N. Tolentino, A. Caneiro *et al.*, J. Synchrotron Radiat. **17**, 93 (2010).

[16]J. Deisenhofer, M. Paraskevopoulos, H.-A. Krug von Nidda, and A. Loidl, Phys. Rev. B **66**, 054414 (2002).

[17]J.-S. Zhou and J. B. Goodenough, Phys. Rev. B **77**, 172409 (2008).

[18]J. F. Mitchell, D. N. Argyriou, C. D. Potter, D. G. Hinks, J. D. Jorgensen, and S. D. Bader, Phys. Rev. B **54**, 6172 (1996).

[19]R. A. Souza, N. M. Souza-Neto, A. Y. Ramos, H. C. N. Tolentino, and E. Granado, Phys. Rev. B **70**, 214426 (2004).

[20]C. Monesi, C. Meneghini, F. Bardelli, M. Benfatto, S. Mobilio, U. Manju, and D. D. Sarma, Phys. Rev. B **72**, 174104 (2005).

[21]A. Y. Ramos, N. M. Souza-Neto, H. C. N. Tolentino, O. Bunau, Y. Joly, S. Grenier, J.-P. Itié, A.-M. Flank, P. Lagarde, and A. Caneiro, EPL **96**, 36002 (2011).

[22]L. Morales, J. Rodriguez-Carvajal, and A. Caneiro, J. Alloy Compd. **369**, 97 (2004).

[23]L. Morales, A. Caneiro, and M. James, Physica B **385**, 415 (2006).

[24]L. Morales, R. Zysler, and A. Caneiro, J. Solid State Chem. **181**, 1824 (2008).

[25]L. Morales and A. Caneiro, J. Solid State Chem. **170**, 404 (2003).

[26]H. C. N. Tolentino, A. Y. Ramos, M. C. M. Alves, R. A. Barrea, E. Tamura, J. C. Cezar, and N. Watanabe, J. Synchrotron Radiat. **8**, 1040 (2001).

[27]O. Proux, V. Nassif, A. Prat, O. Ulrich, E. Lahera, X. Biquard, J. Menthonnex, and J. Hazemann, J. Synchrotron Radiat. **13**, 59 (2006).

[28]F. Baudelet, Q. Kong, L. Nataf, J. D. Cafun, A. Congeduti, A. Monza, S. Chagnot, and J. P. Itié, High Press. Res. **31**, 136 (2011).

[29]F. Bridges, C. H. Booth, G. H. Kwei, J. J. Neumeier, and G. A. Sawatzky, Phys. Rev. B **61**, R9237 (2000).

[30]J. I. Igarashi and K. Hirai, Phys. Rev. B **50**, 17820 (1994).

[31]G. Y. Guo, Phys. Rev. B **57**, 10295 (1998).

[32]O. Bunău and Y. Joly, J. Phys.: Condens. Matter **21**, 345501 (2009).

[33]G. Subias, J. Garcia, M. G. Proietti, and J. Blasco, Phys. Rev. B **56**, 8183 (1997).

[34]M. C. Sánchez, G. Subias, J. Garcia, and J. Blasco, Phys. Rev. B **69**, 184415 (2004).